Laser and Particle Beams (2010), *28*, 497–504.

doi:10.1017/S0263034610000492

Interaction of two plasma jets produced successively from Cu target

A. KASPERCZUK,[1] T. PISARCZYK,[1] J. BADZIAK,[1] S. BORODZIUK,[1] T. CHODUKOWSKI,[1] P. PARYS,[1] J. ULLSCHMIED,[2] E. KROUSKY,[3] K. MASEK,[3] M. PFEIFER,[3] K. ROHLENA,[3] J. SKALA,[3] AND P. PISARCZYK[4]

[1]Institute of Plasma Physics and Laser Microfusion, Warsaw, Poland
[2]Institute of Plasma Physics ASCR, v.v.i., Prague, Czech Republic
[3]Institute of Physics ASCR, v.v.i., Prague, Czech Republic
[4]Warsaw University of Technology, ICS, Warsaw, Poland

(RECEIVED 28 February 2010; ACCEPTED 10 July 2010)

Abstract

Our earlier papers demonstrate a very simple method of plasma jet formation, consisting in irradiating a massive planar target of a relatively high atomic number by a partly defocused laser beam. Our present interest is concentrated on interaction of the plasma jet with other media. This paper is aimed at investigations of interaction of two jets launched successively on Cu target. Our attention was paid to the role of radiative cooling in the plasma jet formation. The experiment was carried out at the PALS iodine laser facility. The laser provided a 250-ps (full width at half maximum) pulse with energy of 130 J at the third harmonic frequency ($\lambda_3 = 0.438$ μm). Two successive jets were produced on a massive flat Cu target provided with a cylindrical channel 5 mm long and 400 μm in diameter. Since the focal spot diameter of the laser beam on the target surface was larger than that of the channel (800 μm), the annular irradiation of the target face resulted in creation of the first plasma jet, whereas the second jet was produced by action of the central part of laser beam on the channel wall. Three-frame interferometric system, X-ray streak camera, and a set of ion collectors were used as diagnostic tools.

Keywords: Electron density distribution; Interaction of plasma jets; Ion collectors; Target irradiation; X-ray streak camera

INTRODUCTION

Collimated plasma outflows (jets) are a subject of great interest in the study of astrophysical phenomena (Borovsky, 1987; Ryutov *et al.*, 2000; Fleury *et al.*, 2002; Mizuta *et al.*, 2002; Kunzl *et al.*, 2003; Schaumann *et al.*, 2005; Bellan, 2005; Loupias *et al.*, 2007), laser plasma interaction phenomena (Hong *et al.*, 2009), and are of interest also for a new fast ignition concept (Velarde *et al.*, 2005). The first attempts to generate jets relevant to astrophysical observation were made by using the world most powerful lasers (Farley *et al.*, 1999; Shigemori *et al.*, 2000). Conically shaped targets made of different materials were irradiated by five beams of the Nova laser (pulse duration 100 ps, energy of each beam 225 J) or by six beams of the GEKKO-XII laser with the same pulse duration, but the total energy of 500 J. In another high-energy experiment worth mentioning (Lebedev *et al.*, 2002) the convergent plasma flows were created by electrodynamic acceleration of the plasma produced by a conical array of fine wires (a modification of the wire array Z-pinch).

In 2006 we reported a simple method of plasma jet generation, which requires much lower laser energy (10–100 J). It is based on irradiation of a flat massive target with atomic number $Z \geq 29$ ($Z = 29$ corresponds to Cu) by a single partly defocused laser beam (Kasperczuk *et al.*, 2006). Our further investigations of plasma jets were devoted to their optimization from the point of view of laser energy, focal spot radius, and position of the focal point with respect to the target surface, i.e., its location inside or in front of the target (Kasperczuk *et al.*, 2007*a*, 2007*b*, 2007*c*). Recently, our investigations of the mechanisms of the plasma jet creation (Kasperczuk *et al.*, 2009*a*) have shown that the geometry of target irradiation is crucial, the annular target irradiation being necessary for plasma jet formation. Also, recently, we proposed and demonstrated effective formation of a supersonic forward-emitted plasma jet by using a cylindrical channel, which guides and collimates the plasma

Address correspondence and reprint requests to: Tadeusz Pisarczyk, Institute of Plasma Physics and Laser Microfusion, 23 Hery St., 00-908 Warsaw, Poland. E-mail: pisaro@ifpilm.waw.pl

produced from a laser-irradiated thin-foil target (Badziak *et al.*, 2009).

Our present interest is concentrated on interaction of the plasma jet with other media. The first experiment devoted to this matter concerned interaction of the plasma jet with ambient gases (Kasperczuk *et al.*, 2009*b*). This paper is aimed at investigations of interaction of two successive jets launched on a Cu target, our attention being paid to the role of radiative cooling in the process of plasma jet formation.

EXPERIMENTAL SETUP AND CONDITIONS

The reported experiment was carried out with the use of the PALS iodine laser facility (Jungwirth, 2005). The plasma was generated by a laser beam of diameter of 290 mm, which was focused by means of an aspheric lens with focal length of 600 mm for the third harmonic of the laser radiation used ($\lambda = 0.438$ μm). The following laser parameters for target irradiation have been chosen: laser energy 130 J, focal spot diameter (Φ_L) 800 μm (the focal point being located inside the target), and a pulse duration 250 ps (full width at half maximum).

For studying the plasma evolution a three-frame interferometric system with automatic image processing was used. The diagnostic system was illuminated by the second harmonic of the iodine laser. The delay between subsequent frames was set to 3 ns.

The diagnostic system also included streaked-slit X-ray imaging. Streaked images of plasma X-ray emission were recorded by KENTECH low magnification X-ray streak camera mounted in a side view. The temporal and spatial resolutions of X-ray images were 30 ps and 50 μm, respectively. To avoid registration of visible plasma radiation, the recording channel of the camera was covered with 8.5 μm of Mylar and 40 nm of Al. In this arrangement, the transmission was negligible for photons of energy less than 0.8 keV, and amounted to about 20% for photons of 1.3 keV. As the laser-produced plasma exhibits such a high temperature only during the laser pulse period, the streak camera registered radial distribution changes of the plasma radiation in the vicinity of the target surface.

Characteristics of the plasma ion emission were measured by four ion collectors mounted 39 cm off the target in horizontal plane at angles 0°, 5°50°, 11°30°, and 17° to the laser beam axis. Location of the diagnostics in the experimental set-up is shown in Figure 1.

To obtain two successive jets we used the massive flat Cu target with a cylindrical channel of length 5 mm and diameter of 400 μm. In such a case, the convergent laser beam irradiated both the target surface and the cylindrical wall of the channel. Since the focal spot diameter of the laser beam on the target surface was larger than that of the channel, the annular irradiation of the target mouth resulted in production of *the first plasma jet*, whereas *the second plasma jet* was generated by action of the central part of laser beam on the channel wall. We expected that, due to longer path of flight, the second plasma jet originating inside the channel would be delayed in time in relation to the first one. The process of

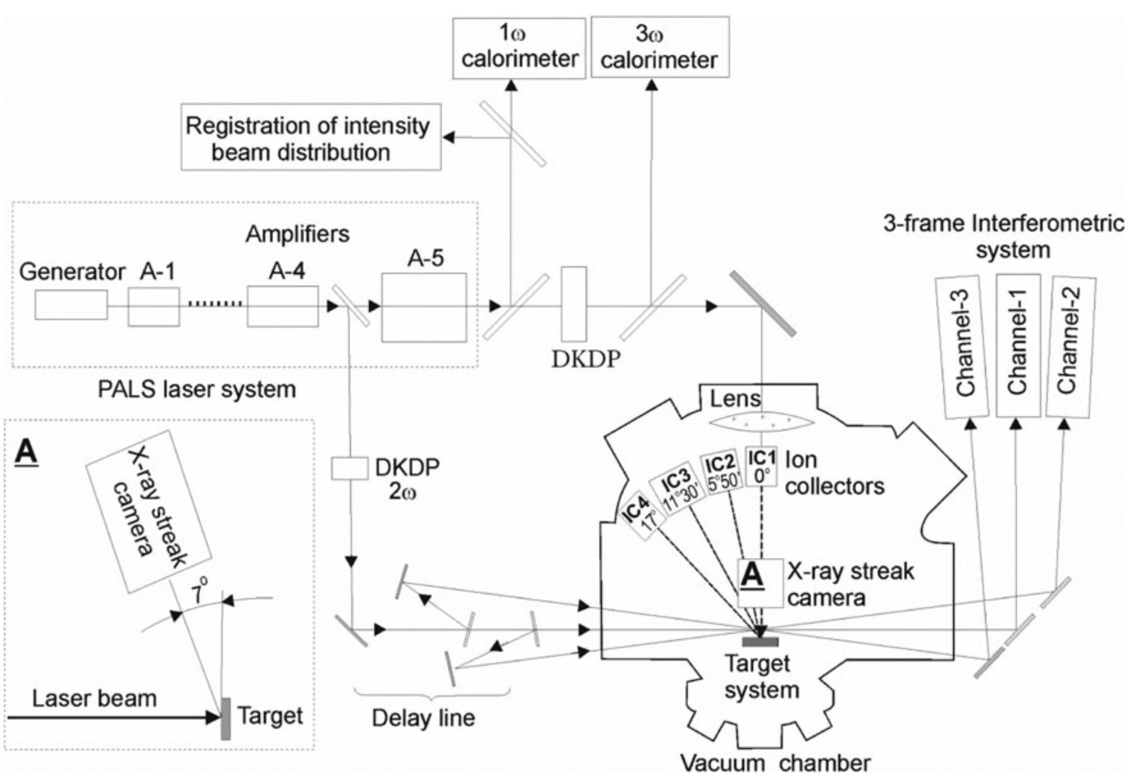

Fig. 1. Experimental set-up.

https://doi.org/10.1017/S0263034610000492 Published online by Cambridge University Press

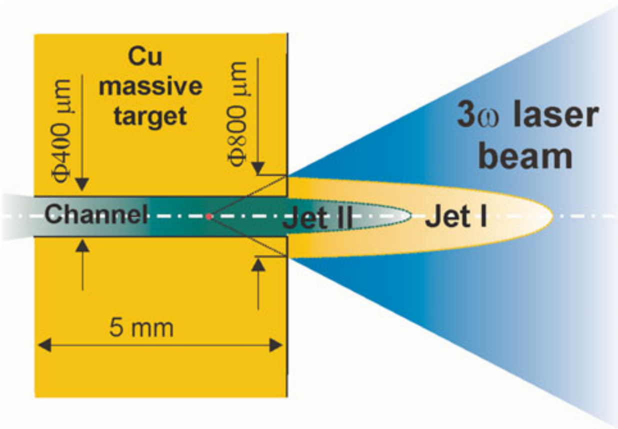

Fig. 2. (Color online) Illustration of the way of creation of two successive plasma jets.

creation of the both of plasma jets is shown schematically in Figure 2.

EXPERIMENTAL RESULTS

The differences in the initial plasma configurations between the targets without and with a channel are well seen in the diagrams of plasma X-radiation, obtained from the streak camera measurements. Their typical examples are presented in Figure 3. The Abel inversion was used to get radial X-ray radiation intensity distributions from the registered streaked images. The plasma X-ray emission intensity distributions are normalized to unity, 0.05 being the step of the adjacent equidensity lines. In Figure 3a, the typical plasma X-ray radiation intensity distribution in the case of the plasma jet launched on a flat massive Cu target without a channel is shown. Its annular form, which is conserved for the whole time of plasma emission, corresponds to the target irradiation geometry being necessary for the plasma jet formation (Kasperczuk *et al.*, 2009*a*). The gas (iodine) laser PALS tends to generate a central depression in the intensity distribution. This is becoming more pronounced with increasing laser energy. In spite of a reasonably small first harmonic intensity depression in the center of the laser beam cross-section before its focusing (not more than 10%), the resulting third harmonic central depression can be much deeper. Thus, the PALS laser beam properties exhibit the annular target irradiation geometry causing part of the generated plasma to collide on the axis.

For the target with a channel of diameter of 400 μm, in spite of the annular target irradiation, a substantial part of laser radiation entered the channel. Thus, the annular profile of laser intensity distribution was partly constrained by the cylindrical hole, the irradiated ring at the target face was narrower, and hence the intensity of plasma radiation was lower (see Fig. 3b). However, after about 1 ns from the streak start, a central narrow streak appeared. It corresponds to the jet coming out from the channel. One can see that X-ray radiation intensity of the central jet is higher than that of the ambient cylindrical plasma at the same time. It witnesses that the

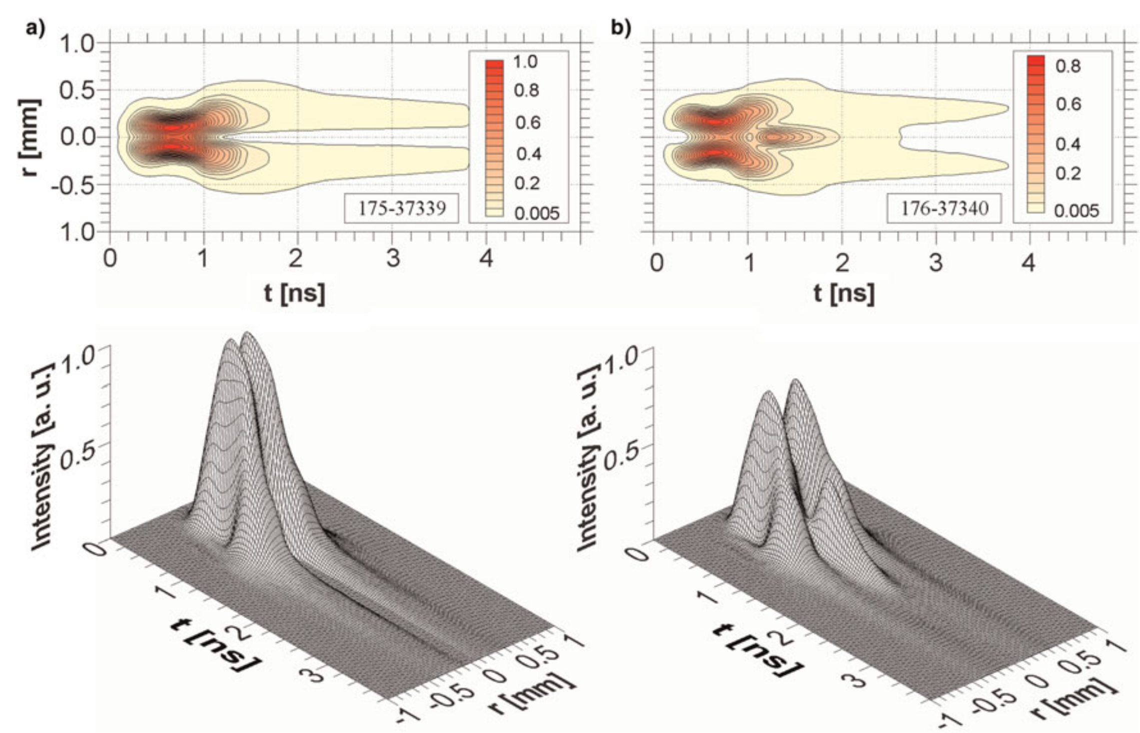

Fig. 3. (Color online) Equidensitograms and spatial distributions of intensities of plasma x-radiation for the targets without (**a**) and with the channel (**b**).

https://doi.org/10.1017/S0263034610000492 Published online by Cambridge University Press

temperature of the central plasma jet is considerably higher than that of the external plasma. Such a difference in temperature of the two plasmas seems to be natural, and expected, since the plasma originating from the target face expands freely, while the expansion of the plasma inside the channel is radially limited. As a result, the pressure in the center of the first plasma jet increases, which leads to a big change in configuration of the whole plasma stream.

The influence of the second plasma jet on the first one can be studied by means of laser interferometry. The two sequences of interferograms corresponding to the targets without and with the cylindrical channel are shown in Figure 4. In the case of the target without the channel (Fig. 4a), the typical plasma jet forming is observed. The cylindrical channel changes the plasma jet configuration, as illustrated by interferograms in Figure 4b. On the basis of these interferograms, the electron density distributions of the plasmas were computed (Fig. 5). In the electron equidensitograms presented there, the outer plasma contour corresponds to the electron equidensity line of 10^{18} cm^{-3}, whereas the distance between adjacent lines is equal to 5×10^{18} cm^{-3}.

These results clearly demonstrate the differences in plasma outflow launched on the targets without and with the channel. In the first case, the plasma jet is produced directly by the laser beam action, and at 10 ns it reaches its final length of about 5 mm and diameter of 300 μm (full width at half maximum). In the other case, the plasma stream has initially a conical form with an apex angle of about 11°. Only after 10 ns a jet-like plasma shape is seen. It means that the plasma jet originating from the channel disturbs the normal process of plasma jet creation.

The channel plasma outflow propagating inside the first plasma jet not only prevents formation of the convergent plasma stream, but causes its divergent expansion. Therefore, instead of the plasma jet, a conically shaped plasma sheath is observed. Depression in the electron density inside the plasma cone suggests that the main factor causing this transformation is a relatively high temperature of the plasma flowing from the channel. The divergent plasma stream lasts until the plasma outflow from the channel stops. Later on, a jet-like form of the plasma stream constitutes very fast (see Fig. 5b at 10 ns).

The electron distributions in Figure 5b prove that in the period of interaction of the two jets the plasma is emitted mainly inside a conical shell. The conically shaped plasma sheath structure is also witnessed by the investigation of the ion fluxes emitted from the plasma. In Figure 6, the time-resolved signals of the ion current integrated over charge states of plasma ion species from four ion collectors viewing the plasma from different angles are plotted for the targets without and with the channel. One can see that for the plasma jet configuration (target without a channel) most of the ions are emitted along the axis (at an angle of 0°). In the other case, the biggest amount of ions is registered by the ion collector placed at an angle of 5°50°. This angle corresponds very well to one-half of the cone apex angle of plasma emission seen in Figure 5b at $t = 7$ ns.

To obtain a divergent plasma configuration lasting for longer times, the amount of plasma flowing from the channel should be enlarged. A simple way on how to do it appears to be to close the second end of the channel. It would prevent the plasma fast escape and increase its mass due to the plasma produced at the bottom of the hole. In our experiment, a Cu slab was used as a stopper. The result of this procedure is seen in Figure 7. The plasma outflow is divergent for the whole observation period. One can also see that in this case the angle of plasma emission is larger.

The above experimental results answer a fundamental question: influence of the radiative cooling on the plasma jet forming at the PALS experiments. The numerical modeling results of the plasma jet creation, presented in many papers (Farley *et al.*, 1999; Mizuta *et al.*, 2002; Nicolai *et al.*, 2006), have shown that radiative cooling is a dominant mechanism in the collapse of plasma on the axis. Depending on the density and temperature, radiation can cool a plasma jet, allowing the jet to collapse to a smaller radius and higher density.

The theoretical analysis of the jet formation presented in the paper by Nicolai *et al.* (2006) says that for the plasma

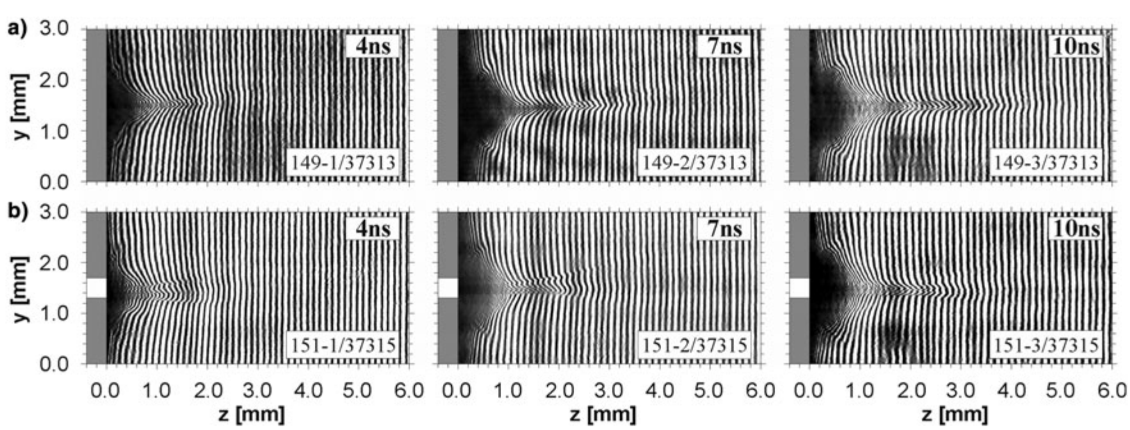

Fig. 4. Sequences of interferograms illustrative of the differences in plasma configuration for the targets without (**a**) and with the cylindrical channel (**b**).

https://doi.org/10.1017/S0263034610000492 Published online by Cambridge University Press

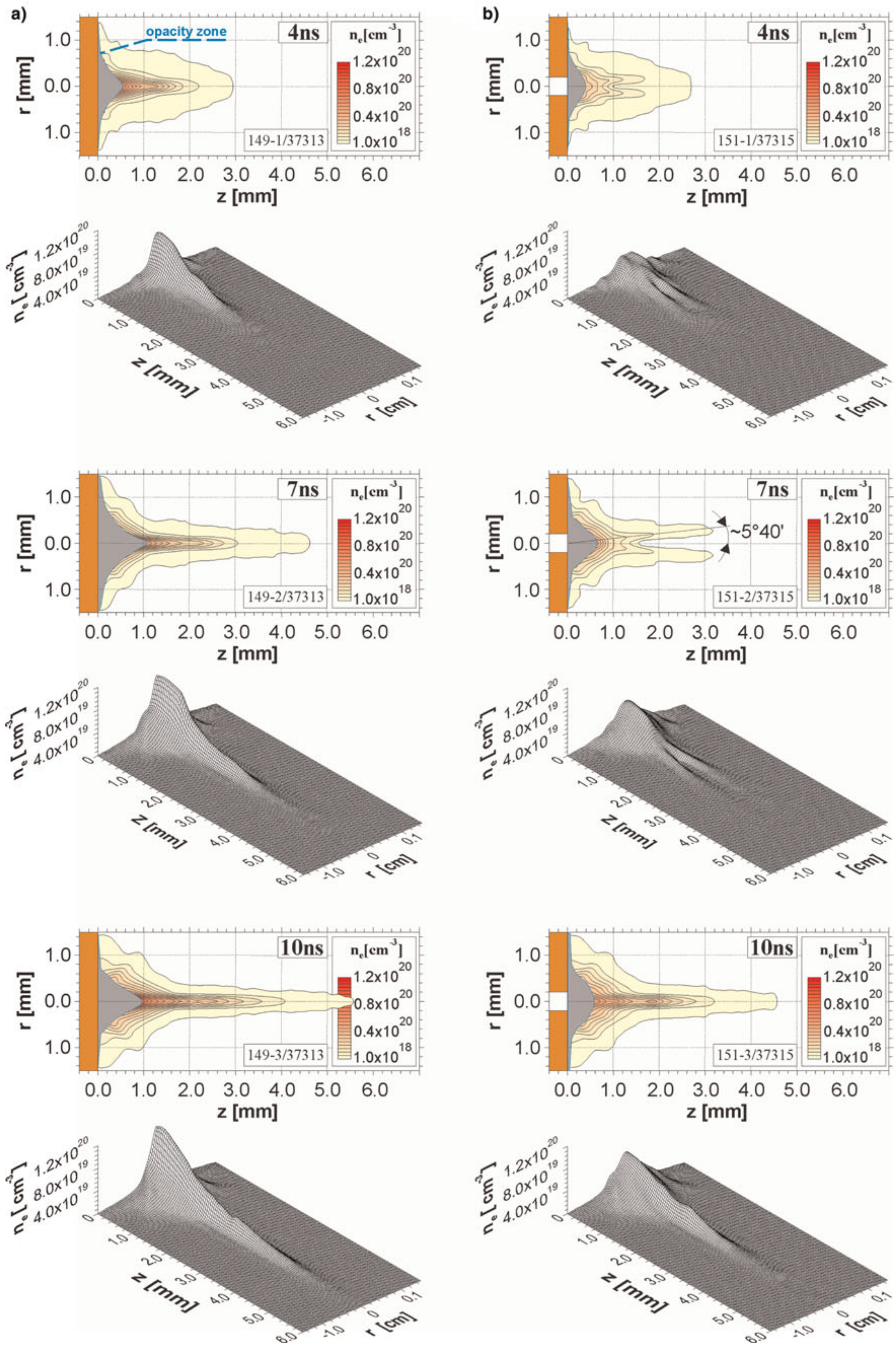

Fig. 5. (Color online) Sequences of electron density distributions in forms of equidensitograms and spatial distribution corresponding to: (**a**) the target without a channel and (**b**) the target with an opened channel. The focal spot diameter is 800 μm.

https://doi.org/10.1017/S0263034610000492 Published online by Cambridge University Press

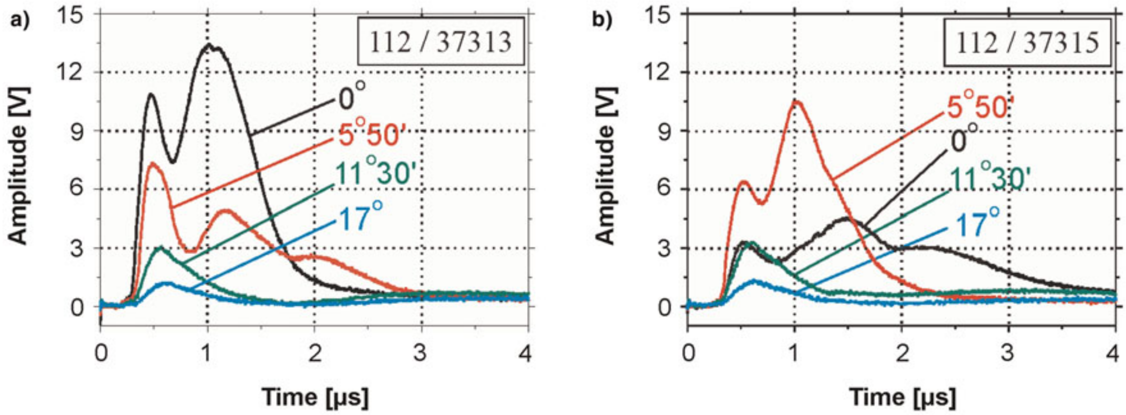

Fig. 6. (Color online) The time-resolved signals of the ion current from the four ion collectors viewing the plasma from different angles: 0°, 5°50', 11°30', and 17° for the targets without (**a**) and with a channel (**b**).

jet to be formed, the characteristic hydrodynamic time (t_h) associated with the plasma expansion should be longer than the time of radiative cooling (t_r). The characteristic hydrodynamic time is the ratio of the focal spot radius R_L and the ion acoustic velocity, while the radiative cooling time is the ratio of the plasma thermal energy and the power of radiative losses. The ratio of t_h/t_r is proportional to the factor $\Phi_L T^{-1} Z_m^{1/2} n_e$, therefore, the radiative effects are more important in a plasma of a larger size Φ_L, a smaller temperature T, a higher average ion charge Z_m, and a higher electron density n_e. For the rough parameters of this experiment, i.e., $Z_m = 15$, $T = 100$ eV, and $n_e = 10^{22}$ cm^{-3} (between the critical density and the ablation front, that is around the launching zone), the hydrodynamic time and

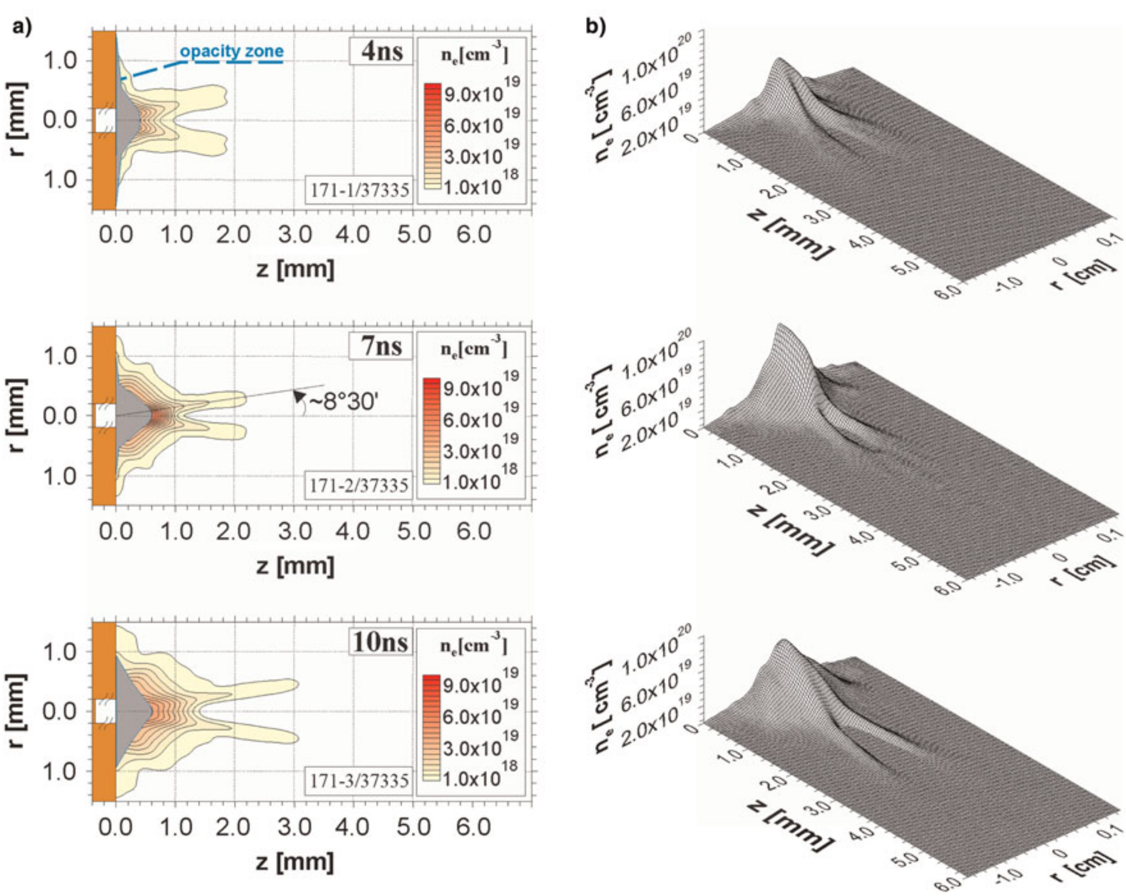

Fig. 7. (Color online) Sequence of electron density distributions in forms of equidensitograms (**a**), and spatial distributions (**b**) corresponding to the closed channel.

https://doi.org/10.1017/S0263034610000492 Published online by Cambridge University Press

the radiation cooling time are estimated to be $t_h \sim 6$ ns and $t_r \sim 0.9$ ns, respectively. It means that, in spite of the second jet action, such a very fast radiative cooling of the expanding plasma should ensure the plasma collapse on the axis. Thus, instead of a divergent plasma stream, a standard plasma jet should be observed. Moreover, the conical configuration of the plasma stream exists for a long time, considerably longer than the radiative cooling time. Transformation of the conical form of the plasma stream into the plasma jet, seen in Figure 4b at 10 ns, occurs when the outflow of second plasma jet stops. So, we can conclude that the conical form of the plasma stream lasts so long as the second plasma jet interacts with the first plasma jet. A block of the second end of the channel elongates the second plasma jet outflow time and interaction of the plasma jets lasts longer time. The conical configuration of the plasma outflow is here preserved for the whole observation time, as it is seen in Figure 7.

Although our interest was focused on explanation of the role of radiative cooling in the process of plasma jet forming, it seems that the mutual interaction of the two plasma jets can deliver interesting information about hot plasma features.

Our experiment presents a relatively simple way of production and interaction of two independent plasma jets. Although in this experiment both the jets were made of the same material, this method creates possibility of using different materials of the jets, when the target face and the channel wall are built from various materials. There is also possibility of modification the channel dimensions and shape to get different mutual relations between the jets, such as a delay between them, ratio of plasma amounts into jets, difference in their velocities and the like. It allows us study a mixing process of two plasmas. Besides, the interaction of two plasma jets makes it possible to create other plasma stream configurations, like a cylindrical pipe or a conically shaped plasma shell.

CONCLUSIONS

According to the theoretical analyses, in which the radiative cooling should play a dominant role in the plasma jet forming, it was anticipated that the additional plasma heating by the second jet action ought not to have changed the typical jet-like plasma configuration. However, it turned out that the radiative cooling is not as effective as it follows from the theoretical predictions. It confirms our earlier suggestion (Kasperczuk *et al.*, 2009*a*) that there is one additional mechanism taking part in the plasma jet forming toward the two such mechanisms considered so far, namely the *annular irradiation* and the *plasma radiative cooling*. Based on numerical simulations, the influence of the plasma *expansion regime* was identified: in the case of Cu, the *planar* expansion regime is taking place and in the case of plastic, it is the *spherical* one. However, the contribution of these mechanisms toward the plasma jet production seems to depend on the target irradiation conditions. Our earlier experiments at PALS laser system have proved that the decisive role in the plasma jet forming plays the annular target irradiation. However, this mechanism acts properly only in the case of target materials with atomic number $Z \geq 29$. If the target is made of low-Z materials like plastic or Al, no plasma jets are observed despite the fact that the laser intensity distribution is the same. If the target irradiation is homogeneous or exhibits only a small depression, the planar Cu plasma expansion should dominate in the plasma jet forming. In this case, the plasma radiative cooling can play an important role by decelerating the Cu plasma during the laser pulse and creating better conditions for the planar plasma expansion. In the case of the plastic plasma, the two contradictory mechanisms are involved, namely the annular target irradiation and the spherical character of plastic plasma expansion. Influence of the latter appears to be stronger and, in consequence, no plasma jet is produced.

REFERENCES

Badziak, J., Pisarczyk, T., Chodukowski, T., Kasperczuk, A., Parys, P., Rosiński, M., Wołowski, J., Krousky, E., Krasa, J., Mašek, K., Pfeifer, M., Skala, J., Ullschmied, J., Velyhan, A., Dhareshwar, L.J., Gupta, N.K., Torrisi, L. & Pisarczyk, P. (2009). Formation of a supersonic laser-driven plasma jet in a cylindrical channel. *Phys.Plasmas* **16**, 114506-1/114506-4.

Bellan, P.M. (2005). Miniconference on astrophysical jets. *Phys. Plasmas* **12**, 058301-1/058301-8.

Borovsky, J.E. (1987). Double layers and plasma-wave resistivity in extragalactic jets: cavity formation and radio-wave emission. *Laser Part. Beams* **5**, 169–175.

Farley, D.R., Estabrook, K.G., Glendinning, S.G., Glenzer, S.H., Remington, B.A., Shigemori, K., Stone, J.M., Wallance, R.J., Zimmerman, G.B. & Harte, J.A. (1999). Stable dense plasma jets produced at laser power densities around 10^{14} W/cm^2. *Phys. Rev. Lett*. **83**, 1982–1985.

Fleury, X., Bouquet, S., Stehle, C., Koenig, M., Batani, D., Benuzzi-Mounaix, A., Chieze, J-P., Grandjouan, N., Grenier, J., Hall, T., Henry, E., Lafon, J-P., Leygnac, S., Malka, V., Marchet, B., Merdji, H., Michaut, C. & Thais, F. (2002). A laser experiment for studying radiative shocks in astrophysics. *Laser Part. Beams* **20**, 263–268.

Hong, W., He, Y., Wen, T., Du, H., Teng, J., Qing, X., Huang, Z., Huang, W., Liu, H., Wang, X., Huang, X., Zhu, Q., Ding, Y. & Peng, H. (2009). Spatial and temporal characteristics of X-ray emission from hot plasma driven by a relativistic femtosecond laser pulse. *Laser Part. Beams* **27**, 19–26.

Jungwirth, K. (2005). Recent highlights of the PALS research program. *Laser Part. Beams* **23**, 177–182.

Kasperczuk, A., Pisarczyk, T., Borodziuk, S., Ullschmied, J., Krousky, E., Masek, K., Rohlena, K., Skala, J. & Hora, H. (2006). Stable dense plasma jets produced at laser power densities around 10^{14} W/cm^2. *Phys. Plasmas* **13**, 062704-1/062704-8.

Kasperczuk, A., Pisarczyk, T., Borodziuk, S., Ullschmied, J., Krousky, E., Masek, K., Pfeifer, M., Rohlena, K., Skala, J. & Pisarczyk, P. (2007*a*). The influence of target irradiation conditions on the parameters of laser-produced plasma jets. *Phys. Plasmas* **14**, 032701-1/032701-4.

Kasperczuk, A., Pisarczyk, T., Borodziuk, S., Ullschmied, J., Krousky, E., Masek, K., Pfeifer, M., Rohlena, K., Skala, J. & Pisarczyk, P. (2007*b*). Interferometric investigations of influence of target irradiation on the parameters of laser-produced plasma jets. *Laser Part. Beams* **25**, 425–433.

Kasperczuk, A., Pisarczyk, T., Badziak, J., Miklaszewski, R., Parys, P., Rosinski, M., Wolowski, J., Stenz, CH., Ullschmied, J., Krousky, E., Masek, K., Pfeifer, M., Rohlena, K., Skala, J. & Pisarczyk, P. (2007*c*). Influence of the focal point position on the properties of a laser-produced plasma. *Phys. Plasmas* **14**, 102706-1/102706-8.

Kasperczuk, A., Pisarczyk, N.N., Demchenko, S.YU., Gus'kov, M., Kalal, M., Ullschmied, J., Krousky, E., Masek, K., Pfeifer, M., Rohlena, K., Skala, J. & Pisarczyk, P. (2009*a*). Experimental and theoretical investigations of mechanisms responsible for plasma jet formation at PALS. *Laser Part. Beams* **27**, 583–591.

Kasperczuk, A., Pisarczyk, T., Nicolai, PH., Stenz, CH., Tikhonchuk, V., Kalal, M., Ullschmied, J., Krousky, E., Masek, K., Pfeifer, M., Rohlena, K., Skala, J., Klir, D., Kravarik, J., Kubes, P. & Pisarczyk, P. (2009*b*). Investigations of plasma jet interaction with ambient gases by multi-frame interferometric and X-ray pinhole camera systems. *Laser Part. Beams* **27**, 115–122.

Kunzl, TH., Lichters, L. & Meyer-ter-Vehn, J. (2003). Large-amplitude plasma waves and 2 omega p emission driven by laser-generated jets in overdense plasma layers. *Laser Part. Beams* **21**, 115–122.

Lebedev, S.V., Chittenden, J.P., Beg, F.N., Bland, S.N., Ciardi, A., Ampleford, D., Hughes, S., Haines, M.G., Frank, A., Blackman, E.G. & Gardiner, T. (2002). Laboratory astrophysics and collimated stellar outflows: The production of radiatively cooled hypersonic plasma jets. *Astrophys. J.* **564**, 113–119.

Loupias, B., Koenig, M., Falize, E., Bouquet, S., Ozaki, N., Benuzzi-Mounaix, A., Vinci, T., Michaut, C., Rabec Ie Goahec, M., Nazarov, W., Courtois, C., Aglitskiy, Y., Faenov, YA. & Pikuz, T. (2007). Supersonic-jet experiments using a high-energy laser. *Phys. Rev. Lett*. **99**, 265001.

Mizuta, A., Yamada, S. & Takabe, H. (2002). Numerical analysis of jest produced by intense laser. *Astrophys. J.* **567**, 635–642.

Nicolai, PH., Tikhonchuk, V.T., Kasperczuk, A., Pisarczyk, T., Borodziuk, S., Rohlena, K. & Ullschmied, J. (2006). Plasma jets produced in a single laser beam interaction with a planar target. *Phys. Plasmas* **13**, 062701-1/062701-8.

Ryutov, D.D., Drake, R.P. & Remington, B.A. (2000). Criteria for scaled laboratory simulations of astrophysical MHD phenomena. *Astrophys. J. Suppl. Series* **127**, 465–468.

Shigemori, K., Kodama, R., Farley, D.R., Koase, T., Estabrook, K.G., Remington, B.A., Ryutov, D.D., Ochi, Y., Azechi, H., Stone, J. & Turner, N. (2000). Experiments on radiative collapse in laser-produced plasmas relevant to astrophysical jets. *Phys. Rev. E* **62**, 8838–8841.

Schaumann, G., Schollmeier, M.S., Rodriguez-Prieto, G., Blazeviz, A., Brambrink, E., Geissel, M., Korostiy, S., Pirzadeh, P., Roth, M., Rosmej, M.B., Faenov, A.YA., Pikuz, T.A. Tsigutkin, K., Maron, Y., Tahir, N.A. & Hoffmann, D.H.H. (2005). High energy heavy ion jets emerging from laser plasma generated by long pulse laser beams from the NHELIX laser system at GSI. *Laser Part. Beams* **23**, 503–512.

Velarde, P., Ogando, F., Eliezer, S., Martinez-Val, J.M., Perlado, J.M. & Murakami, M. (2005). Comparison between jet collision and shell impact concepts for fast ignition. *Laser Part. Beams* **23**, 43–46.